







Original Research Article

Photocatalytic degradation of malachite green dye under UV light irradiation using calcium-doped ceria nanoparticles

Ibrahim A. Amar^{a,b*} , Hebatallah M. Harara^a, Qamrah A. Baqul^a, Mabroukah A. Abdul Qadir^a , Fatima A. Altohamia^a , Mohammed M. Ahwidi^a , Ihssin A. Abdalsamed^a, Fatema A. Saleh^a

^a Department of Chemistry, Faculty of Science, Sebha University, Sebha, Libya

^b Central Laboratory at Sebha University, Sebha, Libya

ARTICLE INFORMATION

Received: 22 June 2019

Received in revised: 12 July 2019

Accepted: 21 July 2019

Available online: 6 September 2019

DOI:

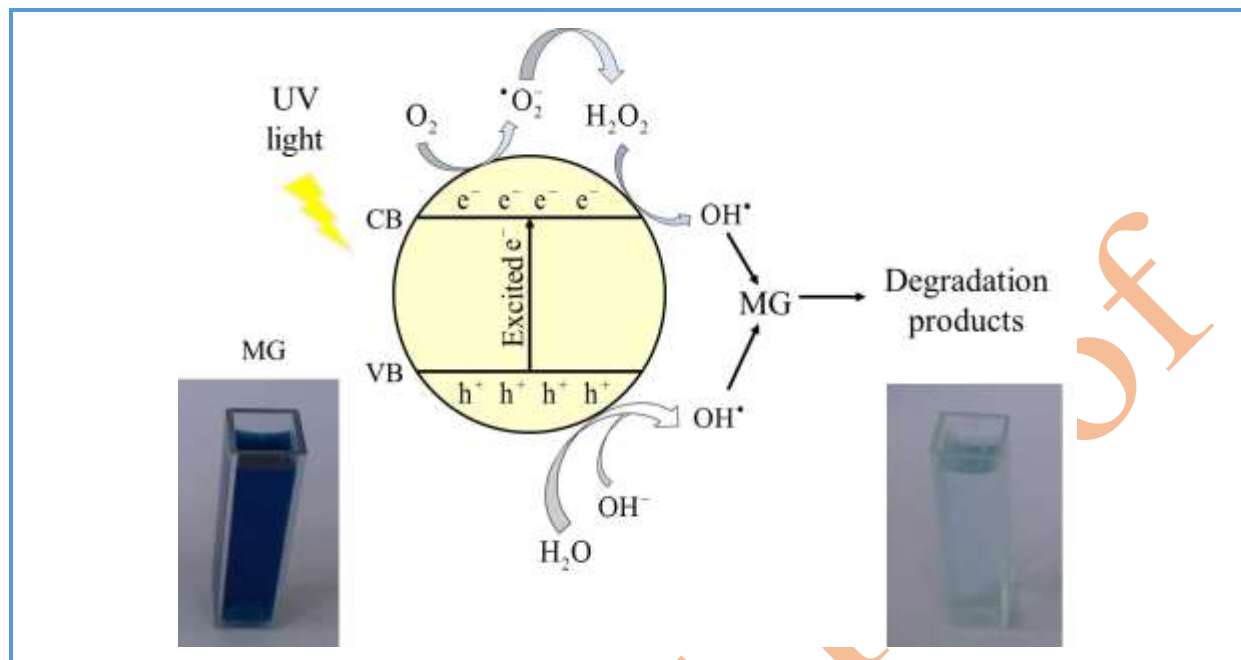
KEYWORDS

Dye photodegradation
Nanostructured materials
Doped ceria catalyst
Semiconductor
Optical properties

ABSTRACT

In this study, photocatalytic activity of Ca-doped ceria (CDC) for malachite green (MG) degradation was investigated. CDC was successfully synthesized via co-precipitation method using ammonium oxalate as a precipitating agent. CDC was characterized using Fourier transform infrared spectroscopy (FTIR), powder X-ray diffraction (XRD), UV-Vis spectroscopy, and scanning electron microscopy (SEM). The band gap energy (E_g) of CDC was found to be 3.96 eV. In addition, the factors affecting the photodegradation of MG including; irradiation time, photocatalyst dosage, initial dye concentration, and solution temperature were studied. The results revealed that CDC could degrade approximately 93% of MG dye at the concentration of 6 mg/L, irradiation time of 90 min, photocatalyst dosage of 0.1 g, and solution temperature of 35 °C. The obtained results indicate that CDC is a promising material for the photocatalytic applications and can be used to eliminate very toxic dyes such as MG.

Graphical Abstract



Introduction

Water pollution by synthetic dyes has become one of the greatest worldwide environmental issues as they pose a considerable threat to both human health and aquatic life [1]. Malachite green (MG), a cationic triphenylmethane dye, has found widespread applications as colouring agent in various industries including; textile (such as silk and wool), food, paper, and leather [2, 3]. It has also been used for the production of ceramics, defend against bacterial infections, and treating scratches on fish bodies in agricultural industry [3]. However, it has been reported that this dye is highly toxic, mutagenic, carcinogenic, and persistent [2]. Therefore, eliminating such a very toxic dye before being discharged into water body is of environmental importance.

Over the last few years, various techniques have been developed to eliminate organic dyes from water environments including, coagulation-sedimentation [4], membrane filtration [5], photocatalysis [6, 7], and

adsorption [8–10]. Among these methods, photodegradation is attracted much attention because it has the ability to decompose and convert a wide range of dangerous contaminants including organic and inorganic compounds into safe by-products [3, 11]. In addition, photocatalysis on the surfaces of semiconductors is regarded as one of the efficient and green solutions for solving serious environmental issues [12–14]. In this process, electron/hole (e^-/h^+) pairs are produced in the conduction (CB) and valence bands (VB) when semiconductor materials are illuminated with light of suitable energy [15]. The generated e^-/h^+ pairs will migrate to the surface of semiconductor particles and produce very reactive radicals (such as OH^\bullet and $^{\bullet}O_2^-$) by the reaction with the surrounding H_2O and O_2 molecules. The combination of reactive oxygen radicals with valence band holes will degrade the dye molecules in the contaminated water [12]. This means that the generated e^-/h^+ pairs contribute significantly in the redox reactions and producing the final products [14].

Cerium oxide (CeO_2), ceria, is an n-type semiconductor with band gap energy (E_g) of about 3.19 eV [16, 17]. In recent years, cerium oxide (CeO_2) nanoparticles (CNPs) have drawn lots of attention due to their remarkable chemical and physical properties including, excellent oxygen release/storage ability, high surface area, low dimensionality, low cost compared to noble metal catalyst, strong absorption of the light in the UV region and chemical, and photocorrosion resistance [6, 16, 18, 19]. Therefore, CNPs and their nanocomposites have found applications in different areas such as optical devices [20] solid oxide fuel cells (SOFCs) [21], ammonia synthesis [22, 23], photocatalysis [6, 24], UV absorbents and filters [25, 26], and gas sensors [16]. In addition, the properties of cerium oxide are greatly enhanced by controlling the oxygen vacancies within the oxide structure using the substitution strategy. It has been reported that the catalytic activities of CeO_2 were significantly improved by the substitution of Ce atom by lower oxidation state elements (M^{+2} or M^{+3}) [27]. In this regard, several substituted CeO_2 nanomaterials have been employed for dye photodegradation applications. Recently, Murugan *et al.* [7] used alkaline metal ion (Mg, Ca, Sr, Ba) doped ceria NPs for the photodegradation of methylene blue (MB). In one study, Yue and Zhang [28] used Fe-doped ceria for the photocatalytic degradation of methylene blue. In another study, Gnanam *et al.* [6] have successfully synthesized (Cd, Pd) doped ceria NPs for the photocatalytic degradation of Rhodamine B (RhB) and Congo red (CR) dyes. In addition, Maria Magdalane *et al.* [29] have synthesized CeO_2/CdO multi-layered nanoplatelet arrays and investigated their photocatalytic degradation of malachite green (MG). Among the aforementioned dopants, Ca^{+2} is of practical importance because it is readily available and economically viable

[30]. To the best of our knowledge, there is no report on malachite green degradation using Ca-doped ceria (CDC) as a photocatalyst. Based on this discussion, the main focus of the present study is to synthesize CDC and to investigate their photocatalytic degradation for a very toxic cationic dye namely malachite green.

Experimental

Materials and methods

Malachite green ($\text{C}_{23}\text{H}_{25}\text{ClN}_2$) was purchased from Riedel-de Haën. Ammonium cerium (IV) nitrate ($(\text{NH}_4)_2\text{Ce}(\text{NO}_3)_6$) was purchased from VWR Prolabo BDH Chemicals. Calcium nitrate ($\text{Ca}(\text{NO}_3)_2 \cdot 4\text{H}_2\text{O}$) and Ammonium oxalate ($(\text{NH}_4)_2\text{C}_2\text{O}_4 \cdot \text{H}_2\text{O}$) were purchased from T-Barker Lab Chemicals. The chemicals were used as received without any further purification.

Synthesis of $\text{Ce}_{0.8}\text{Ca}_{0.2}\text{O}_{2-\delta}$ catalyst

A photocatalyst composed of calcium-doped ceria ($\text{Ce}_{0.8}\text{Ca}_{0.2}\text{O}_{2-\delta}$, CDC) was synthesized via a co-precipitation method [31]. In a typical procedure, the required amounts of $(\text{NH}_4)_2\text{Ce}(\text{NO}_3)_6$ and $\text{Ca}(\text{NO}_3)_2 \cdot 4\text{H}_2\text{O}$ were dissolved in deionized water. Then, 0.3 M ammonium oxalate solution (precipitating agent) was added dropwise to the mixed solution under vigorous stirring until a complete precipitation occurs. Then, the resulted white precipitate was stirred for 1 h to get a homogenous mixture that was vacuum filtered before being washed several times with deionized water and ethanol. The obtained precipitate was dried overnight at 80 °C. Finally, pale-yellow fine powder of CDC was obtained after firing the dried precipitate in air at 600 °C for 2 h.

Characterization

Philips- PW 1800 diffractometer with CuK α radiation ($\lambda = 1.54186 \text{ \AA}$) was used to record the X-ray diffraction (XRD) pattern of CDC. The XRD data of the most intense peaks was used to estimate the lattice parameters (a), volume of the unit cell (V_{cell}), crystallite size (D), the X-ray density (ρ_{XRD}) and the specific surface area (S_{XRD}) of CDC using Equations 1 to 5, respectively [32, 33].

$$a = d_{hkl} \sqrt{h^2 + k^2 + l^2} \quad (1)$$

$$V_{\text{cell}} = a^3 \quad (2)$$

$$D = \frac{0.9 \lambda}{(\beta \cos \theta)} \quad (3)$$

$$\rho_{\text{XRD}} = \frac{ZM}{N_A V_{\text{cell}}} \quad (4)$$

$$S_{\text{XRD}} = \frac{6000}{D \cdot \rho_{\text{XRD}}} \quad (5)$$

where, d is the interplanar distance, hkl are the Miller indices, β is the full width at half maximum (FWHM) of the peak in radiance, θ is the Bragg angle, λ is the wavelength of the X-ray, N_A is the Avogadro's number, Z is the number of molecules per formula unit ($Z = 4$ for fluorite system) and M is the molecular weight of the sample.

LEO 1430PV scanning electron microscope (SEM) was used to characterize the morphology of CDC. The Fourier transform infrared (FT-IR) spectrum of the photocatalyst (CDC) was recorded using Nicolet 380 spectrometer using KBr pellet technique in the wavenumber range of 400-4000 cm^{-1} . UV-Vis spectrophotometer (Evolution 300, Thermo Electronic Corporation) was used to record the absorption spectrum of CDC using quartz cuvettes of 1 cm in length within the wavelength of 200 to 500 nm. To do this, CDC powder (1 mg) was dispersed into 25 mL of ethanol by ultrasonication for 30 min [26]. The optical band gap energy (E_g) of CDC can be estimated by plotting $(\alpha h\nu)^2$ against $h\nu$ for direct transitions, as

described by the following equation [17];

$$(\alpha h\nu)^n = B(h\nu - E_g) \quad (6)$$

where, $h\nu$ is the photon energy (eV), α is the absorption coefficient and B is a constant relative to the material. The value of n equals 2 for direct transitions and $\frac{1}{2}$ for indirect transitions. In addition, Einstein's photoelectric effect formula the E_g of CDC according to the following Equation [34, 35];

$$E_g (\text{eV}) = \frac{1240}{\lambda}$$

where, λ is wavelength corresponding to absorption peak of CDC.

Photocatalytic Degradation Test

A 100 mg/L stock solution of MG was prepared by dissolving the weight amount of MG into the required volume of deionized water. The working solutions with the desired concentrations were prepared by diluting the MG stock solution using deionized water. To carry out the photodegradation test, a certain amount of CDC powder was added to 25 mL flasks containing 20 mL of MG solution. Then, the reaction mixture was shaken in the dark for 30 min to ensure adsorption/desorption equilibrium before being irradiated for predetermined time under UV light ($\lambda = 366 \text{ nm}$) using UV lamp, 8 W, (CAMAG, Switzerland). After each photodegradation experiment, the reaction mixture was centrifuged for 5 min at speed of 4000 rpm. Then, a single beam UV-Vis spectrophotometer (GENESYS 10 UV, Thermo Electronic Corporation) was used to measure the residual concentration of MG at a maximum wavelength (λ_{max}) of 617 nm. To investigate photocatalytic activity of CDC, the experiments were conducted under different operational conditions including; irradiation time (0-180 min), initial dye concentration (2-10 mg/L), photocatalyst dosage (0.04-0.14 g) and dye solution temperature (25-45 °C). The

photocatalysis experiments were carried out in triplicate and the percentage degradation of MG was estimated using the following equation [36];

$$\% \text{ Degradation} = \frac{A_0 - A_t}{A_0} \times 100 \quad (8)$$

where, A_0 is the initial absorbance of MG dye solution and A_t is the absorbance of MG dye solution after photodegradation for certain time t .

Results and Discussion

Characterization

Figure 1 displays the XRD pattern of CDC. As shown, a single phase of CDC was obtained

when the corresponding precursors were calcined in air at 600 °C for 2 h. As seen in Figure 1, all the observed peaks were well indexed to cerium oxide (CeO_2) with a cubic fluorite structure (JCPDS card No. 34-0394). The structural parameters values of CDC were estimated using the XRD data of the most intense peaks. The calculated values of lattice constant ($a=b=c$), the crystallite size (D), unit cell volume (V_{cell}), the X-ray density (ρ_{XRD}) and the specific surface area (S_{XRD}) were found to be $5.3050 \pm 0.0348 \text{ \AA}$, $14.08 \pm 6.00 \text{ nm}$, $149.31 \pm 2.94 \text{ \AA}^3$, 6.76 g/cm^3 and $63.04 \text{ m}^2/\text{g}$, respectively. Moreover, the specific surface area is an important parameter which can affect the material's properties such as photochemical efficiency, physical property and chemical reactivity [32].

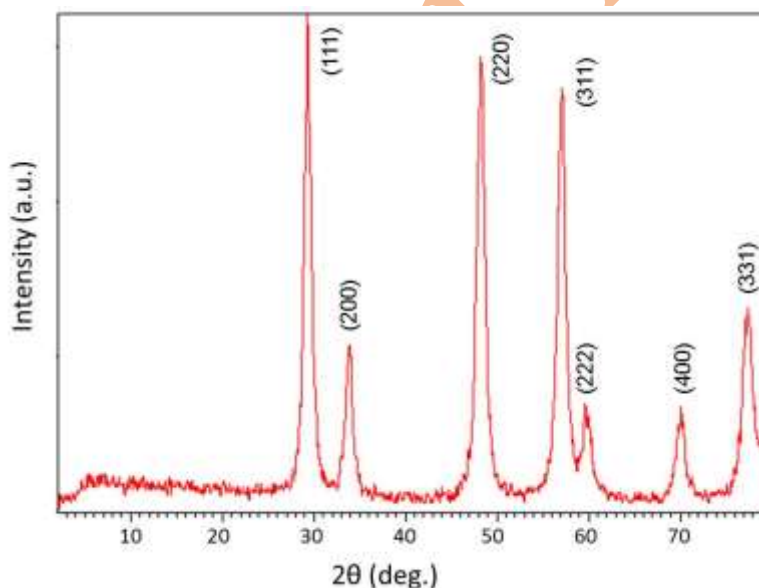


Figure 1. Powder X-ray diffraction pattern of $\text{Ce}_{0.8}\text{Ca}_{0.2}\text{O}_{2-\delta}$ powder

Figure 2 displays the FT-IR spectrum of CDC powder within the wavenumber ranging from 400 to 4000 cm^{-1} . As shown, the absorption band located at 486 cm^{-1} is assigned to the stretching vibration of Ce–O bond [37]. The bands located within the wavenumber range of 713–1175 cm^{-1} are accredited to C–O stretching

vibration [7]. The band located around 1423 cm^{-1} is attributed to C–H bending vibration [38]. The weak band observed at 2612 cm^{-1} is assigned to C–H stretching vibration. This is an indication of organic compounds adsorption onto the surface of CDC [37]. The broad band located 3402 cm^{-1} and the weak band observed

at 1793 cm^{-1} are attributed to stretching and bending vibrations of O–H bond, respectively [6].

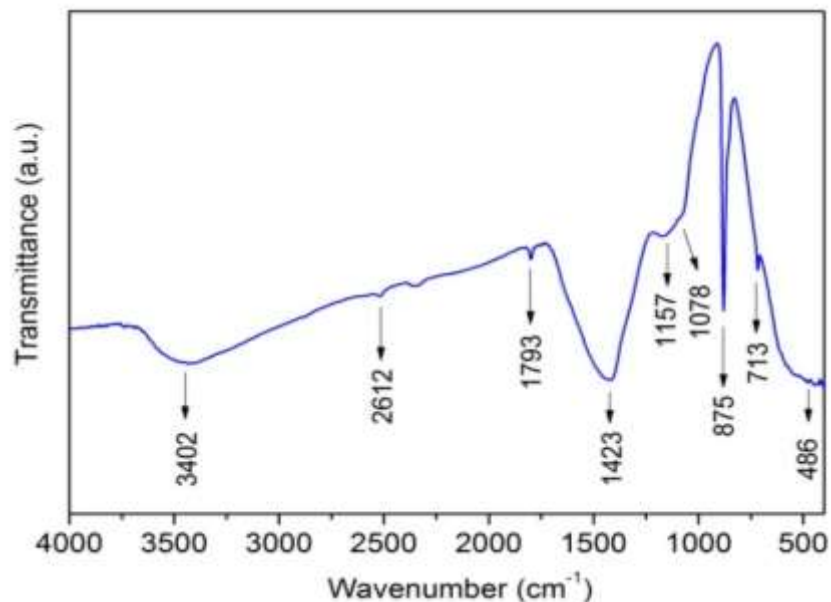


Figure 2. FT-IR spectrum of $\text{Ce}_{0.8}\text{Ca}_{0.2}\text{O}_{2-\delta}$ powder

The morphology of CDC surface was investigated using scanning electron microscope (SEM) and the result is showing in Figure 3. As shown from SEM image, the surface morphology of CDC consists of small particles which are agglomerated and then form

aggregates. These agglomerates ($\sim 30\ \mu\text{m}$) are formed because of two reasons. First, the small particles (in nano scale) are energetically more stable in the agglomeration configuration. Second, the agglomeration of the small particles allows for crystal growth [26].

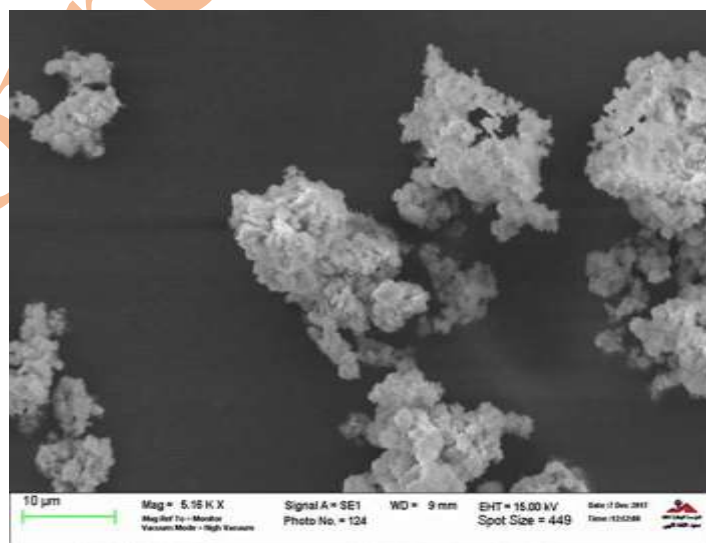


Figure 3. SEM image of $\text{Ce}_{0.8}\text{Ca}_{0.2}\text{O}_{2-\delta}$ powder

The energy band structure feature is one of the important factors that play an important role in determining the photocatalytic activities of the semiconductor [13]. The optical property of CDC was investigated using UV-Vis technique. **Figure 4a** displays the UV-Vis absorption spectrum of CDC, dispersed in ethanol, in the range of wavelength between 200 to 500 nm. As can be seen, the CDC sample exhibit a strong absorption peak between 225 and 325 nm, with a maximum value at approximately 269 nm.

Figure 4b depicts the plot of $(\alpha h\nu)^2$ against $h\nu$ (Tauc plot) from which the band gap energy (E_g) of CDC was determined. The E_g value is estimated from the intersection of the extrapolated linear portion with x -axis at which the absorption is zero (see **Figure 4b**). The E_g value of the prepared photocatalyst (CDC) was found to be 3.96 eV. This value is higher than those reported previously by *Truffault et al.* [26] for pure CeO_2 (3.20 eV) and 20% mol Ca-doped CeO_2 (3.36 eV).

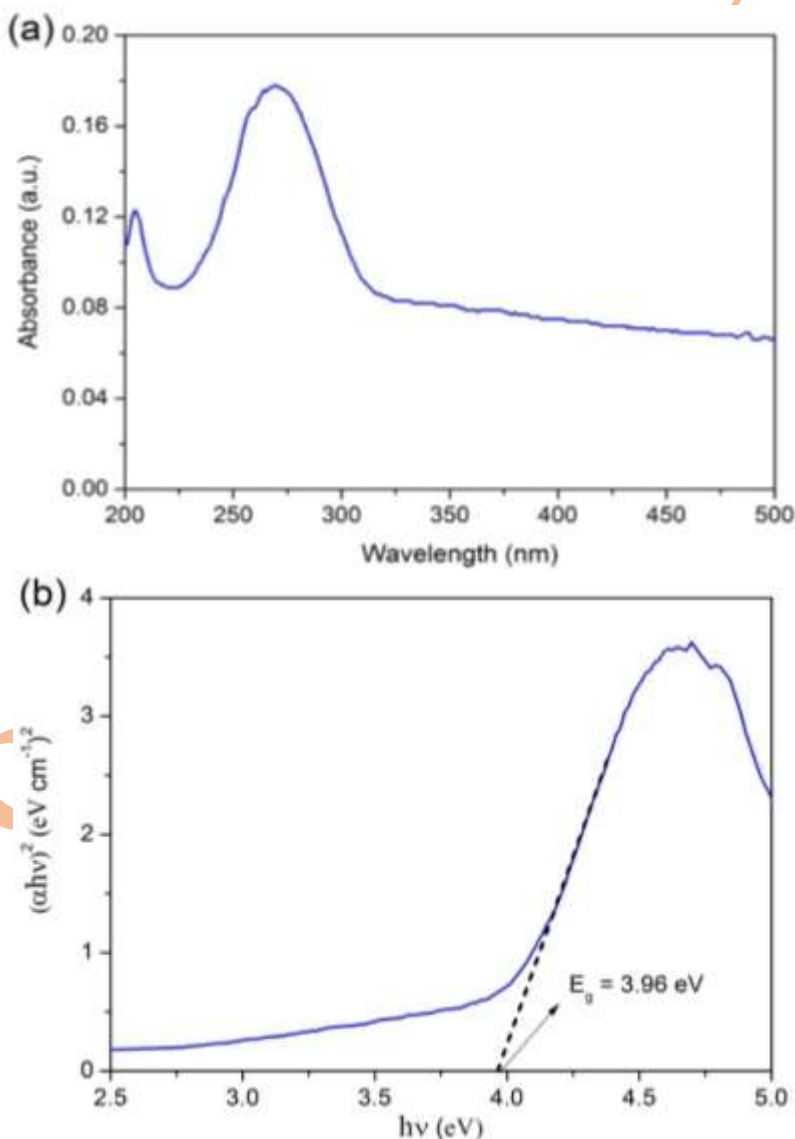


Figure 4. a) UV-Vis absorption spectrum of $Ce_{0.8}Ca_{0.2}O_{2-\delta}$, b) Tauk plot*Photocatalytic activity of CDC*

As mentioned earlier, the photocatalytic activity of CDC was investigated under different operational conditional including; irradiation time, initial concentration of MG, photocatalyst dosage and solution temperature. Figure 5a represents the UV-Vis spectra of MG dye (10 mg/L) at different irradiation time (0-180 min) and photocatalyst dosage of 0.1 g. As can be seen, the peak intensity (at 617 nm) decreased with increasing the irradiation time and reaching a low intensity at irradiation time of 90 min. It also is to be noted that, no observable degradation was observed when MG dye was

subjected to UV irradiation for 180 min in the absence the CDC. This indicates that the observed degradation of MG was a result of the photocatalytic activity of CDC. Figure 5b shows the percentage degradation of MG as a function of irradiation time (0-180 min). As shown, the CDC catalyst was able to degrade almost 50% of MG dye in the first 5 min of irradiation time. In addition, there was a slight increase in the percentage degradation of MG as the irradiation was increased. The maximum value percentage degradation (65.69%) was attained at 90 min irradiation time after which a slight decrease in the percentage degradation was observed.

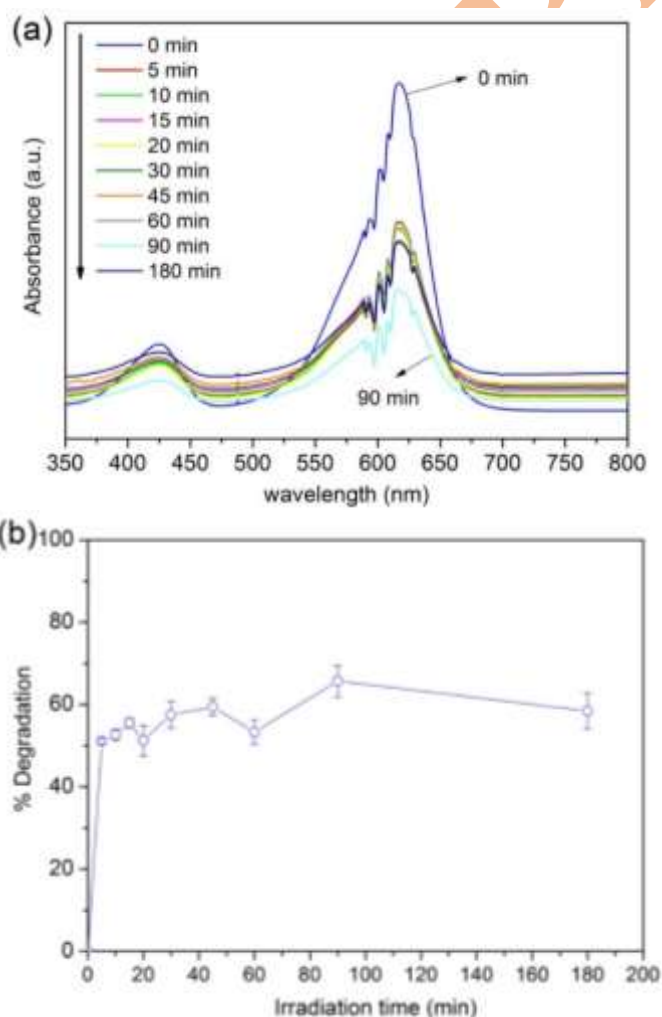


Figure 5. a) UV-Vis spectra changes during the photodegradation of MG, b) Effect of irradiation time on the percentage degradation of MG

To determine the effect of initial MG concentration, the experiment was conducted at different MG concentration (2-10 mg/L) and the other experimental conditions were kept under fixed values (irradiation time of 90 min and photocatalyst dosage of 0.1 g). The effect of MG initial concentration on the percentage degradation is shown in Figure 6. As can be seen, the percentage degradation changed from 70.29% at MG concentration of 2 mg/L to 84.53% when the MG initial concentration was increased to 6 mg/L. This increase in percentage degradation could be explained based on the fact that by increasing the MG initial concentration, the MG molecules quantities per volume unit will increase and

enhancing the collision probability between the MG molecules and oxidizing species which in turn resulted in an increase in the photodegradation percentage of MG dye [39]. However, by further increasing MG initial concentration above 6 mg/L, a decrease in the percentage degradation was observed reaching a minimum value of about 65.69% at an initial concentration of 10 mg/L. This could be due to that fact that more light will be absorbed by dye molecules rather than by the photocatalyst at high initial dye concentration. This in turn will lead to a reduction in the formation of hydroxyl (OH^\bullet) and superoxide ($\text{O}_2^{\bullet-}$) radicals and consequently decreasing the photocatalyst activity [40].

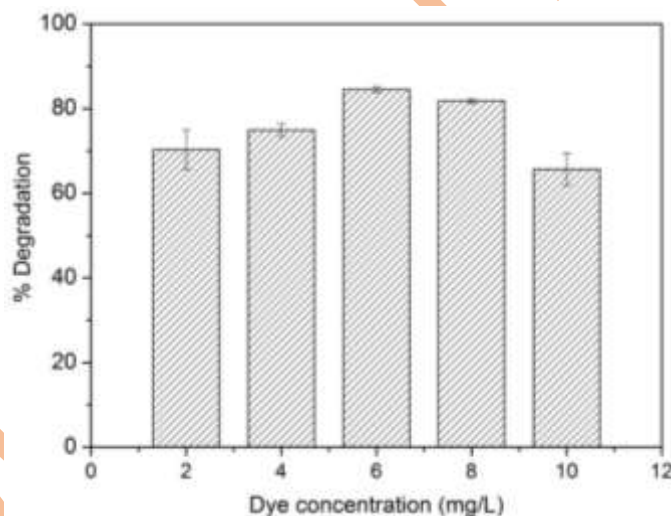


Figure 6. Effect of the initial concentration on the percentage degradation of MG

The effect of the photocatalyst (CDC) amount on the percentage degradation was investigated by changing the CDC dosage from 0.04 g to 0.14 g. For this, the experiment was carried out at irradiation time of 90 min, initial MG concentration of 6 mg/L and room temperature and the result is shown in Figure 7. As demonstrated, the percentage degradation of

MG remains almost at a constant value (~75%) when the CDC amount was increased from 0.04 to 0.08 g. In addition, an increase in the percentage degradation of about 84.53% was observed as the CDC was increased to 0.1 g. This could be due to the increase in the number of photocatalyst active sites which in turn resulted in enhancing OH^\bullet radicals' production and

consequently increasing the percentage degradation of MG [40, 41]. However, by further increasing the CDC amount above the optimum value (0.1 g), the percentage degradation decreased approximately to a constant value. This observed decrease in the percentage

degradation might be due the fact that, increasing the photocatalyst amount will result in increasing the turbidity of the suspension and leading to a reduction in the penetration of UV light as a result of light scattering effect [41, 42].

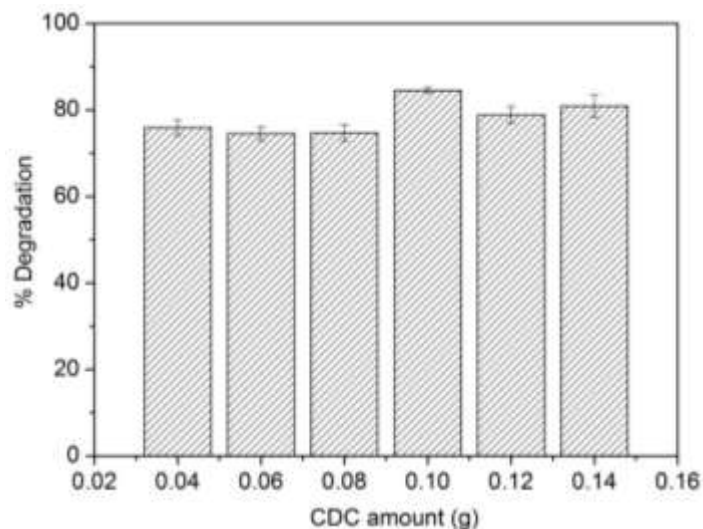


Figure 7. Effect of photocatalyst amount on the percentage degradation of MG

Figure 8 displays the percentage degradation of MG as a function of dye solution temperature. This experiment was conducted at various solution temperatures (25, 35, and 45 °C), irradiation time of 90 min, photocatalyst dosage of 0.1 g and initial MG concentration of 6 mg/L. As shown, there was a slight increase in the percentage degradation was observed as the solution temperature was increased from 25 °C (89.51%) to 35 °C (92.52%). In addition, the percentage degradation of MG decreased

slightly when solution temperature was increased to 45 °C (90.86%). This indicates that a solution temperature of 35 °C seems to be the best temperature in the present work. Table 1 represents the percentage degradation of MG using different photocatalyst materials [3, 36, 43-45]. As can be seen from the table, the proposed material (CDC) seems to be promising photocatalyst and can be used for the degradation of very toxic dyes.

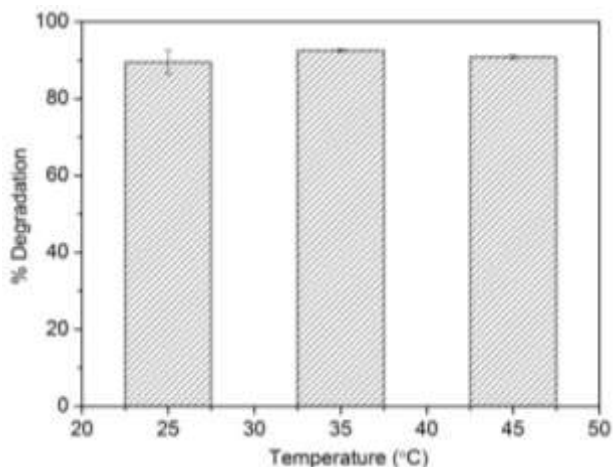


Figure 8. Effect of the solution temperature on the percentage degradation of MG

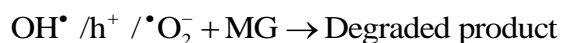
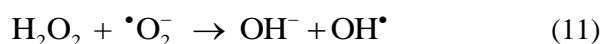
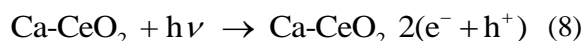
Table 1. Comparison of percentage degradation of MG using different photocatalysts

Photocatalyst	Light source	Lamp power (w)	MG concentration (mg/L)	Degradation (%)	Irradiation time (min)	Reference
SiO ₂	Visible	125	10	100	10	[3]
ZnO	Visible	500	50	67	60	[43]
ZnO-doped LO ^a	Visible	500	50	99	60	[43]
La _{0.7} Ba _{0.3} CoO ₃	Visible	250	10	97	60	[44]
CdO	UV	30	10	76	175	[36]
Ag-CdO	UV	30	10	78	175	[36]
TiO ₂	UV	15	50	100	360	[45]
Ce _{0.8} Ca _{0.2} O _{2-δ}	UV	8	6	93	90	This study

^alanthanide oxide

Figure 9 represents a schematic diagram for the proposed degradation mechanism of MG under UV light irradiation using CDC as a photocatalyst. When the CDC catalyst is irradiated by UV light, holes in the VB will be created as the electrons in the VB got excited and jumped to the CB. These generated holes will react with the surrounding H₂O and producing highly reactive hydroxyl radicals (OH•). In addition, highly reactive oxygen radicals (•O₂⁻) will be produced when the generated electrons (e⁻) react with the surrounding atmospheric oxygen molecules

(O₂). These reactive species are responsible for MG photodegradation [7, 36, 46].



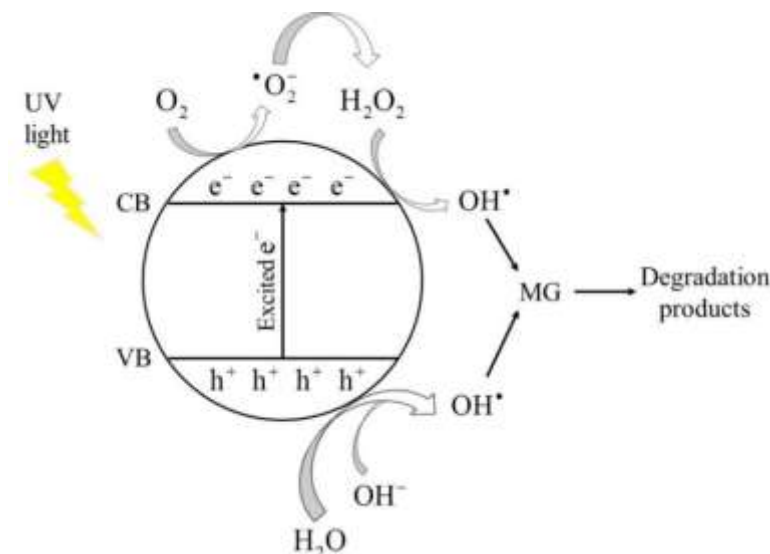


Figure 9. Schematic representation for mechanism of MG photodegradation using CDC as a photocatalyst under UV irradiation

Conclusion

A photocatalyst composed of Ca-doped ceria nanoparticles (CDC) was synthesized *via* coprecipitation method using ammonium oxalate as a precipitating agent. The XRD results revealed that a single phase of CDC with cubic structure was successfully formed. The estimated band gap energy (E_g) value of CDC was found to 3.96 eV. In addition, under the optimum operational conditions (initial dye concentration of 6 mg/L, irradiation time of 90 min, photocatalyst dosage of 0.1 g and solution temperature of 35 °C), approximately 93% of malachite green (MG) dye could be degraded under UV irradiation using CDC NPs as a photocatalyst. The present study reveals that CDC is potentially promising candidate photocatalyst materials for degradation of very toxic synthetic dyes from aqueous environments.

Acknowledgements

The authors are thankful to the Department of Chemistry, Sebha University, Sebha, Libya for


the financial support of this work. The authors also thank the Criminal Investigation Department, Branch Sabha City for FTIR and UV instruments. The authors are grateful to Eng. Asma Marei and Eng. Hussan Kut from the Libyan Petroleum Institute, Tripoli, Libya for performing XRD and SEM analysis.

Disclosure statement

No potential conflict of interest was reported by the authors.

Orcid

Ibrahim A. Amar  0000-0003-2354-0272

Mabroukah A. Abdul Qadir  0000-0003-1674-9211

Fatima A. Altohami  0000-0002-9513-9069

Mohammed M. Ahwidi  0000-0002-8800-668X

References

- [1]. Mousavi M., Habibi-Yangjeh A., Pouran S. R. *J. Mater. Sci. Mater. Electron.*, 2018, **29**:1719

- [2]. Chen Y., Zhang Y., Liu C., Lu A., Zhang W. *Int. J. Photoenergy*, 2012, **2012**:1
- [3]. Mohamed A., Ghobara M. M., Abdelmaksoud M. K., Mohamed G.G. *Sep. Purif. Technol.*, 2019, **210**:935
- [4]. Gallego-Urrea J.A., Hammes J., Cornelis G., Hassellöv M. *NanoImpact.*, 2016, **3-4**:67
- [5]. Dickhout J.M., Moreno J., Biesheuvel P.M., Boels L., Vos W.M.d., Lammertink R.G.H. *J. Colloid Interface Sci.*, 2017, **487**:523
- [6]. Gnanam S., Rajendran V. *J. Alloys Compd.*, 2018, **735**:1854
- [7]. Murugana R., Kashinath L., Subash R., Sakthivel P., Byrappa K., Rajendran S., Ravi G. *Mater. Res. Bull.*, 2018, **97**:319
- [8]. Al-Anber Z.A., Al-Anber M.A., Matouq M., Al-Ayed O.O., Omari N.M.N.M. *Desalination.*, 2011, **276**:169
- [9]. Amar I. A., Sharif A., Alkhalayali M., Jabji M., Altohami F., AbdulQadir M., Ahwidi M.M. *IJEE*, 2018, **9**:247
- [10]. Awini L.A., El-Rais M.A., Etorki A.M., Mohamed N.A., Erhab H.M. *Mater. Focus*, 2018, **7**:1
- [11]. Feizpoor S., Habibi-Yangjeh A., Yubuta K., Vadivelc S. *Mater. Chem. Phys.*, 2019, **224**:10
- [12]. Markovic D., Milovanovic S., Radoicic M., Radovanovic Z., Zizovic I., Saponjic Z., Radetic M. *J. Serb. Chem. Soc.*, 2018, **83**:1379
- [13]. Adepu A.k., Katta V., Venkatathri N. *New. J. Chem.*, 2017, **41**:2498
- [14]. Pirhashemi M., Habibi-Yangjeh A., Pouran S.R. *J. Ind. Eng Chem.*, 2018, **62**:1
- [15]. Ayodhya D., Veerabhadram G. *Mater. Today. Energy.*, 2018, **9**:83
- [16]. Van Dao D., Nguyen T.T.D., Majhi S.M., Adilbish G., Lee H.J., Yu Y.T., Lee I.H. *Mater. Chem. Phys.*, 2019, **231**:1
- [17]. Elahi B., Mirzaee M., Darroudi M., Oskuee R.K., Sadri K., Amiri M.S. *Ceram. Int.*, 2019, **45**:4790
- [18]. Chandar N.K., Jayavel R. *Physica E.*, 2014, **58**:48
- [19]. Channei D., Inceesungvorn B., Wetchakun N., Ukritnukun S., Nattestad A., Chen J., Phanichphant S. *Sci. Rep.*, 2014, **4**:5757
- [20]. Goubin F., Rocquefelte X., Whangbo M.H., Montardi Y., Brec R., Jobic S. *Chem. Mater.*, 2004, **16**:662
- [21]. Yu J.G., Yang B.C., Shin J.W., Lee S., Oh S., Choi J.H., Jeong J., Noh W., An J. *Ceram. Int.*, 2019, **45**:3811
- [22]. Amar I.A., Petit C.T. G., Zhang L., Lan R., Skabara P.J., Tao S.W. *Solid. State. Ionics.*, 2011, **201**:94
- [23]. Amar I.A., Petit C.T.G., Mann G., Lan R., Skabara P.J., Tao S. *Int. J. Hydrogen Energy.*, 2014, **39**:4322
- [24]. Li H., Wang G., Zhang F., Cai Y., Wang Y., Djerdj I. *RSC. Adv.*, 2012, **2**:12413
- [25]. Li R., Yabe S., Yamashita M., Momose S., Yoshida S., Yin S., Sato T. *Solid. State. Ionics.*, 2002, **151**:235
- [26]. Truffault L., Ta M.T., Devers T., Konstantinov K., Harel V., Simmonard C., Andrezza C., Nevirkovets I.P., Pineau A., Veron O., Blondeau J.P. *Mater. Res. Bull.*, 2010, **45**:527
- [27]. Slostowski C., Marre S., Bassata J.M., Aymonier C. *J. Supercrit. Fluids.*, 2013, **84**:89
- [28]. Yue L., Zhang X.M. *J. Alloys Compd.*, 2009, **475**:702
- [29]. Maria Magdalane C., Kaviyarasu K., Judith Vijaya J., Jayakumar C., Maaza M., Jeyaraj B. *J. Photochem. Photobiol., B.*, 2017, **169**:110
- [30]. Banerjee S., Devi P.S., Topwal D., Mandal S., Menon K. *Adv. Funct. Mater.*, 2007, **17**:2847
- [31]. Ma Y., Wang X., Khalifa H.A., Zhu B., Muhammed M. *Int. J. Hydrogen Energy.*, 2012, **37**:19401
- [32]. Soleimani F., Salehi M., Gholizadeh A. *Ceram. Int.*, 2018, **45**:9826.
- [33]. Fu Y.P., Chen S.H., Huang J.J. *Int. J. Hydrogen Energy.*, 2010, **35**:745
- [34]. Matmin J., Jalani M.A., Osman H., Omar Q., Ab'lah N., Elong K., Kasim M.F. *Nanomaterials.*, 2019, **9**:264

- [35]. He H.Y., Lu J. *Sep. Purif. Technol.*, 2017, **172**:374
- [36]. Mandal R.K., Purkayastha M.D., Majumder T.P. *Optik*. 2019, **180**:174
- [37]. Athawale A.A., Bapat M.S., Desai P.A. *J. Alloys Compd.*, 2009, **484**:211
- [38]. Prabakaran D.M.D.M., Sadaiyandi K., Mahendran M., Sagadevan S. *Mat. Res.*, 2016, **19**:478
- [39]. Nezamzadeh-Ejhieh A., Shams-Ghahfarokhi Z. *J. Chem.*, 2013, **2013**:11
- [40]. Saleh R., Djaja N.F. *Superlattices Microstruct.*, 2014, **74**:217
- [41]. Sanna V., Pala N., Alzari V., Nuvoli D., Carcelli M. *Mater. Lett.*, 2016, **162**:257
- [42]. Raja V.R., Karthika A., Kirubahar S.L., Suganthi A., Rajarajan M. *Solid. State. Ionics.*, 2019, **332**:55
- [43]. Josephine G.A.S., Ramachandran S., Sivasamy A. *J. Saudi Chem Soc.*, 2015, **19**:549
- [44]. Zhang C., Hen H., Wang N., Chen H., Kong D. *Ceram. Int.*, 2013, **39**:3685-3
- [45]. Chen C.C., Lu C.S., Chung Y.C., Jan J.L. *J. Hazard. Mater.*, 2007, **141**:520
- [46]. Saikia L., Bhuyan D., Saikia M., Malakar B., Dutta D.K., Sengupt P. *Appl. Catal. A-Gen.*, 2015, **490**:42

How to cite this manuscript: Ibrahim A. Amar*, Hebatallah M. Harara, Qamrah A. Baqul, Mabroukah A. AbdulQadir, Fatima A. Altohami, Mohammed M. Ahwidi, Ihssin A. Abdalsamed, Fatema A. Saleh. Photocatalytic degradation of malachite green dye under UV light irradiation using calcium-doped ceria nanoparticles . *Asian Journal of Nanoscience and Materials*, 2019, x(x), xx-xx. DOI: